“A Boost-Full-Bridge-Type Single-Active-Bridge Isolated AC-DC Converter”

ABSTRACT

A boost-full-bridge (BFB) single-active-bridge (SAB) ac-dc converter is proposed in this paper. The topology has high power density and galvanic isolation, thanks to its high-frequency (HF) transformer link. In addition, it can be easily controlled by using the proposed modulation and control scheme. Furthermore, it is able to block dc-side short-circuit fault current contribution. The converter operation principles are analyzed. Experiment results are also given to show the startup dynamics, steady-state waveforms, and the dc fault blocking capability.

I. INTRODUCTION

The isolated ac-dc converter plays an important role for a wide range of applications, such as: dc distribution, chargers for electric vehicles, adapters for consumer electronics, etc [1]-[6]. A conventional isolated ac-dc converter normally consists of two stages: (a) an ac-dc stage; and (b) an isolated dc-dc stage. However, the two-stage structure can reduce system efficiency, increase system costs and meanwhile lead to a complex gate-driving system. To avoid those problems, one-stage isolated ac-dc topologies have been proposed (see Fig. 1 [7], [8]). For the topology in Fig. 1(a) [7], four-quadrant switch cells are used, which results in difficult switching commutation and increased conduction losses [7], [9]. As for Fig. 1(b) [8], a line-frequency-switched synchronous rectifier is required, which also increases system costs, losses, and control burden. In this paper,

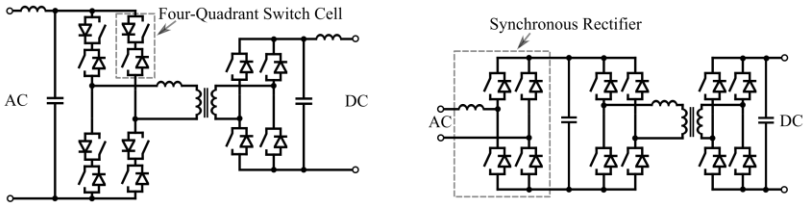

(a) (b)

Fig. 1. Typical one-stage isolated ac-dc converter topologies. (a) Topology proposed in [7]. (b) Topology proposed in [9].

based on the concepts of boost-half-bridge (BHB) converters [10], [11] and single-active bridge (SAB) converters [12], [13], a new type of isolated ac-dc converter is proposed.

II. TOPOLOGY DERIVATION

In [10], [11], a BHB converter is proposed, as shown in Fig. 2(a). A BHB combines a boost converter and a half bridge, and therefore gives a current-fed input port with a terminal inductor L_p, and makes the input current continuous and controllable. Furthermore, by adjusting the duty cycle d_p, the BHB converter is able to provide a variable input voltage v_{tp} [14]. However, this topology is actually unfit for ac-dc applications for the following reasons:

a. Both the high-frequency (HF) transformer and the terminal inductor L_p are connected to the same leg of the BHB. However, only one control freedom (duty cycle d_p) is available. When d_p is adjusted, not only the input current is controlled, but also the HF transformer current i_p is impacted, driven by the asymmetry and the voltage-second imbalance of v_p in each switching period. This leads to a challenging design of a closed-loop controller [15], [16].

b. For ac-dc conversion, both the input current and the duty cycle d_p should be line-frequency sinusoidal at the steady state, resulting in v_p and i_p also containing line-frequency components, which leads to the core saturation or oversize of the HF transformer.

c. Even though the input voltage v_{tp} is adjustable, its polarity has to be positive, or else the control of the BHB will be lost due to its anti-parallel diode.

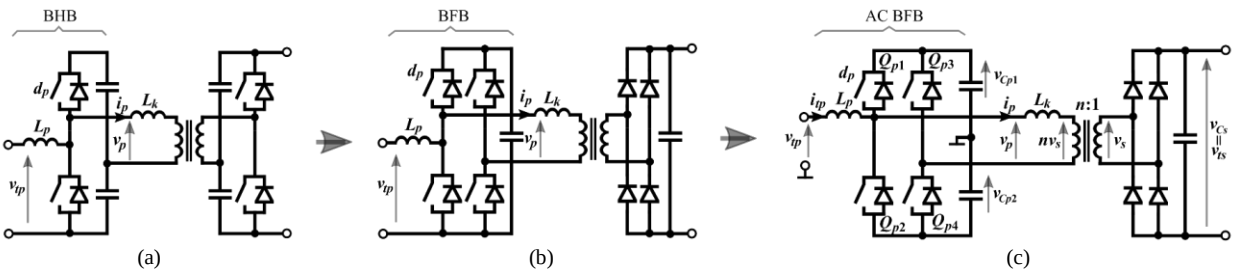

Fig. 2. Topology derivation. (a) BHB-DAB dc-dc converter in [10], [11]. (b) Proposed BFB-SAB dc-dc converter. (c) Proposed BFB-SAB ac-dc converter. (Note: d_p is the duty cycle for the high-side switch.)

For solving these problems, the BHB is extended to boost-full-bridge (BFB) in this paper, as shown in Fig. 2(b). Additionally, a diode bridge is used at the secondary side to reduce the system costs and control complexity. Moreover, by moving the negative input terminal to the neutral of the dc bus [see Fig. 2(c)], the proposed converter is able to handle ac input voltage.

III. OPERATION PRINCIPLES

As introduced in Section II, for the BHB converter in Fig. 2(a), the asymmetrical waveform and voltage-second-imbalance of v_p is the key reason of causing problems. By contrast, for the BFB converter in Fig. 2(c), by using the modulation method in Fig. 3, the voltage-second balance of v_p can be always ensured in each switching period with arbitrary value of the duty cycle d_p. In other words, the dynamics of the input current i_{tp} and the HF transformer current i_p are decoupled.

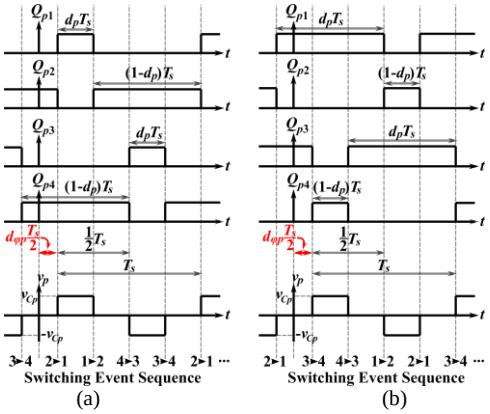

Fig. 3. Modulation method for BFB cell. (a) Waveform for $d_p < 0.5$. (b) Waveform for $d_p > 0.5$. (Note: $d_{\phi p} = |1 - 2d_p|/2$.)

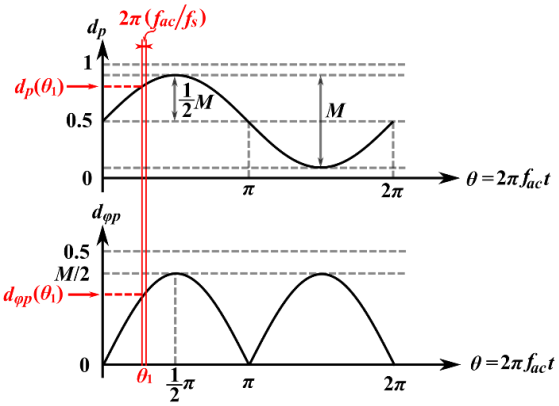

Fig. 4. Steady-state waveforms of d_p and $d_{\phi p}$ in one line-frequency period. (Note: M is the modulation index.)

As shown in Fig. 4, for the proposed ac-dc topology, when the switching frequency is much higher than the line frequency (i.e., $f_s \gg f_{ac} = 50\text{Hz or } 60\text{Hz}$), the duty cycle d_p can be regarded as a constant in each switching period. In other words, the ac-dc operation can be regarded as a smooth shift of the dc-dc operation with different values of d_p in each switching period. The steady-state converter equations (see Table I) can be derived by looking at different stages of the switching

cycle in an analogous way as described in [10]-[13]. The converter dynamics are presented through the experimental results in the next section. A control structure is proposed in Fig. 5, which is almost same as the control of a voltage source converter (VSC) [17]. (Detailed theoretical analysis will be given in the final paper.)

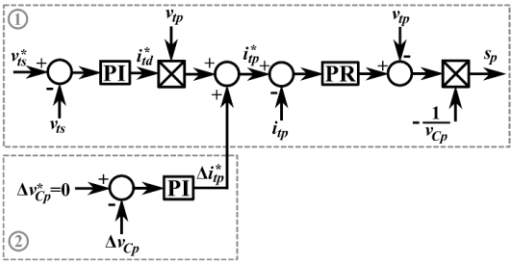

Fig. 5. Control structure for the BFB-SAB ac-dc converter. (Note: PR is the proportional-resonant controller [18]; s_p is the zero-biased duty cycle, i.e. $s_p = d_p - 0.5$; and $\Delta v_{Cp} = v_{Cp1} - v_{Cp2}$.)

TABLE I. STEADY-STATE EQUATIONS

$d_{\varphi p} = \frac{1}{2}\lvert 1 - 2d_p \rvert,\ k = \frac{v_{Cp}}{n v_{Cs}}$
$n v_{Cs} = v_{Cp} \times \begin{cases} (1 - 2d_\varphi) & \text{IF } BM \\ \dfrac{1 - 2d_{\varphi p}}{1 + 2d_\varphi - 2d_{\varphi p}} & \text{IF } DCM \end{cases}$
$d_\varphi = \begin{cases} \frac{1}{2}\left(1 - \frac{1}{k}\right) & \text{IF } BM \\ \frac{1}{2}\left(k(1 - 2d_{\varphi p}) + 2d_{\varphi p} - 1\right) & \text{IF } DCM \end{cases}$
$P = \frac{n v_{Cp} v_{Cs}}{4 f_s L_k} \times \begin{cases} \left(2d_{\varphi p}^2 - \frac{1}{2} + \frac{1}{2k^2}\right) & \text{IF BM} \\ (2d_{\varphi p} - 1)^2 (k - 1) & \text{IF DCM} \end{cases}$
$I_{p,max} = \frac{n v_{Cs}}{2 f_s L_k} \times \begin{cases} (k - 1)\left(\frac{1}{2k} - 2d_{\varphi p} + \frac{1}{2}\right) & \text{IF BM} \\ (k - 1)(1 - 2d_{\varphi p}) & \text{IF DCM} \end{cases}$

IV. EXPERIMENT RESULTS

The converter prototype is shown in Fig. 6, and the experiment results are summarized in Figs. 7 and 8. The close-up and global steady-state waveforms are shown in Figs. 7 and 8(b), respectively. Noticeably, the converter has two different operation modes with different values of the duty cycle [13]: (a) border mode (BM); and (b) discontinuous current mode (DCM). The converter operates in two modes alternatively with the change of the duty cycle [see the 3rd subplot in Fig. 8(b)]. Notably in Fig. 7, the HF transformer voltages v_p and v_s are always symmetrical in each switching period, which means the voltage-second balance is always ensured. Fig. 8(a) shows the startup performance of the converter, which validates the closed-loop control structure. In Fig. 8(c), a dc-side short-circuit fault happens to the converter. The converter detects the fault when the output dc voltage drops to its 66% rated value, and then disables all power switches and blocks the fault. (More detailed analysis of experiment results will be given in the final paper.)

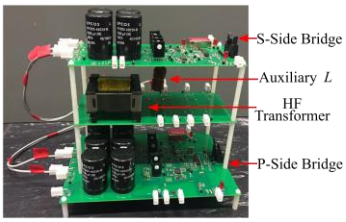

Fig. 6. Prototype of the proposed converter.

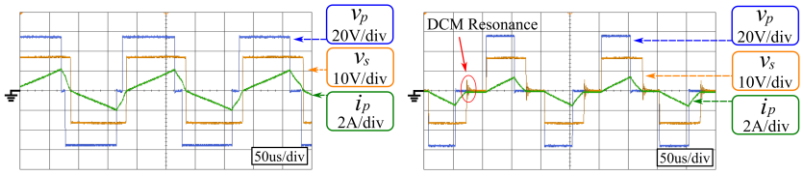

(a) (b)

Fig. 7. Close-up plots of the steady-state waveforms of the HF transformer. (a) Border mode (BM) if $d_\phi > d_{\phi p}$. (b) Discontinuous current mode (DCM) if $d_\phi < d_{\phi p}$.

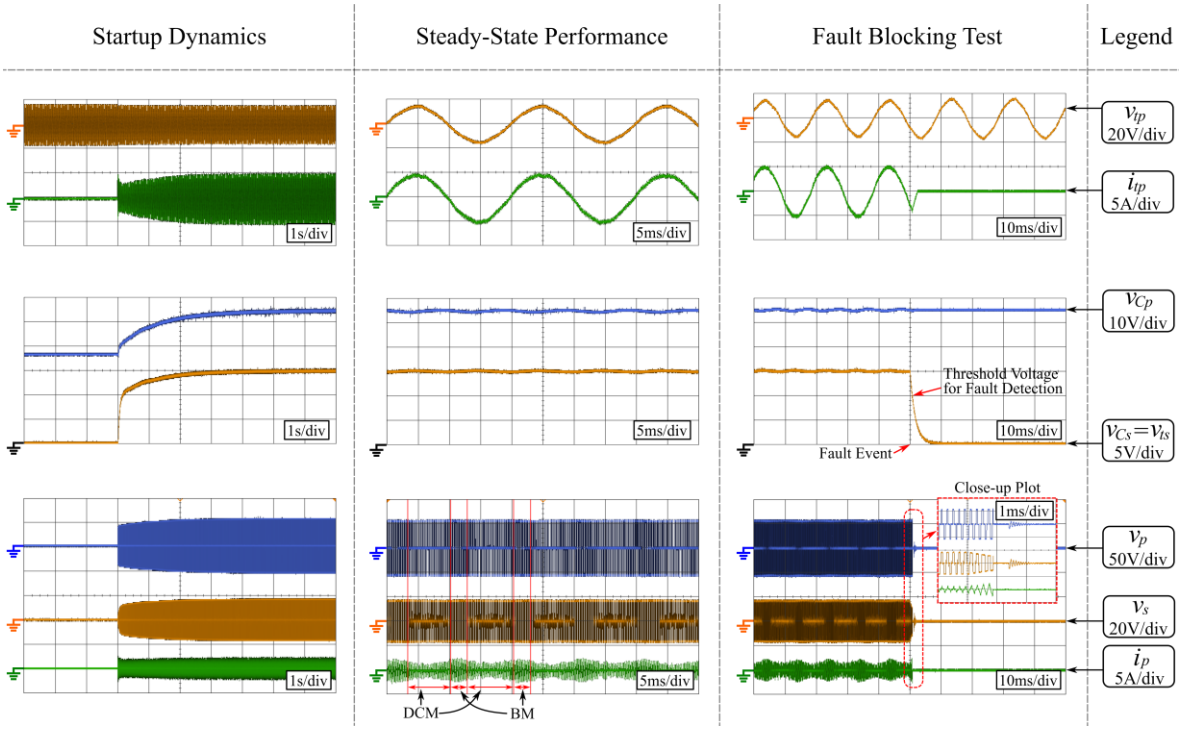

(a) (b) (c)

Fig. 8. Experiment results. (a) Startup dynamics. (b) Steady-state waveforms. (c) Dc-side short-circuit fault blocking test.

IV. CONCLUSIONS and FUTURE WORK

A BFB-type SAB converter has been proposed. The proposed converter inherits benefits of conventional SAB converters, while also achieving ac-dc conversion. Compared with the BHB, the proposed BFB has improved dynamics and an enhanced controllability. Compared with existing single-stage isolated ac-dc converters, the proposed converter can be more easily controlled and analyzed. Modulation scheme and control structure are proposed. Operation principles and experiment results are given. (More detailed results will be shown in the final paper.)

REFERENCES

[1] M.Yilmaz and P. T.Krein, "Review of battery charger topologies, charging power levels, and infrastructure for plug-in electric and hybrid vehicles," *IEEE Trans. Power Electron.*, vol. 28, no. 5, pp. 2151–2169, May 2013.

[2] X. She, A. Q. Huang, and R. Burgos, "Review of solid-state transformer technologies and their application in power distribution systems," *IEEE J. Emerg. Sel. Topics Power Electron.*, vol. 1, no. 3, pp. 186–198, Sep. 2013.

[3] B. Zhao, Q. Song, W. Liu, and Y. Sun, "Overview of dual-active-bridge isolated bidirectional dc-dc converter for high-frequency-link power- conversion system," *IEEE Trans. Power Electron.*, vol. 29, no. 8, pp. 4091–4106, Aug. 2014.

[4] G. AlLee and W. Tschudi, "Edison redux: 380 Vdc brings reliability and efficiency to sustainable data centers," *IEEE Power Energy Mag.*, vol. 10, no. 6, pp. 50–59, Nov./Dec. 2012.

[5] Y. Li, A. Junyent-Ferré, and J. M. Rodriguez-Bernuz, "A three-phase active rectifier topology for bipolar DC distribution," *IEEE Trans. Power Electron.*, vol. 33, no. 2, pp. 1063–1074, Feb. 2018.

[6] B. Yang, F. C. Lee, A. J. Zhang, and G. Huang, "LLC resonant converter for front end dc/dc conversion," in *Proc. IEEE APEC'02, 2002,* pp. 1108–1112.

[7] N. D. Weise, G. Castelino, K. Basu, and N. Mohan, "A single-stage dual-active-bridge-based soft switched ac–dc converter with open-loop power factor correction and other advanced features," *IEEE Trans. Power Electron.*, vol. 29, no. 8, pp. 4007–4016, Aug. 2014.

[8] J. Everts, F. Krismer, J. Van den Keybus, J. Driesen, and J. W. Kolar, "Optimal ZVS modulation of single-phase single-stage bidirectional DAB AC-DC converters," *IEEE Trans. Power Electron.*, vol. 29, no. 8, pp. 3954–3970, Aug. 2014.

[9] H. Qin and J. W. Kimball, "Solid state transformer architecture using ac-ac dual active bridge converter," *IEEE Trans. Ind. Electron.*, vol. 60, no. 9, pp. 3720–3730, Sep. 2012.

[10] H. Li, F. Z. Peng, and J. S. Lawler, "A natural ZVS medium-power bidirectional dc–dc converter with minimum number of devices," *IEEE Trans. Ind. Applicat.*, vol. 39, pp. 525–535, Mar./Apr. 2003.

[11] F. Z. Peng, H. Li, G.-J. Su, and J. S. Lawler, "A new ZVS bi-directional dc-dc converter for fuel cell and battery application," *IEEE Trans. Power Electron.*, vol. 19, no. 1, pp. 54–65, Jan. 2004.

[12] R. W. A. A. D. Doncker, D. M. Divan, and M. H. Kheraluwala, "A three-phase soft-switched high-power-density dc/dc converter for high-power applications," *IEEE Trans. Ind. Appl.*, vol. 27, no. 1, pp. 63–73, Jan./Feb. 1991.

[13] A. Averberg, and A. Mertens, "Characteristics of the single active bridge converter with voltage doubler," *Power Electronics and Motion Control Conference 2008*, pp. 213-220, September 2008.

[14] H. Tao, J. Duarte, and M. Hendrix, "Three-port triple-half-bridge bidirectional converter with zero-voltage switching," *IEEE Trans. Power Electron.*, vol. 23, no. 2, pp. 782–792, Mar. 2008.

[15] S. Jiang, D. Cao, Y. Li, and F. Z. Peng, "Grid-connected boost-half-bridge photovoltaic microinverter system using repetitive current control and maximum power point tracking," *IEEE Trans. Power Electron.*, vol. 27, no. 11, pp. 4711–4722, Nov. 2012.
[16] B. Zhao, Q. Song, W. Liu, and Y. Zhao, "Transient dc bias and current impact effects of high-frequency-isolated bidirectional dc–dc converter in practice," *IEEE Trans. Power Electron.*, vol. 31, no. 4, pp. 3203–3216, Apr. 2016.
[17] R. Srinivasan and R. Oruganti, "A unity power factor converter using half-bridge boost topology," *IEEE Trans. Power Electron.*, vol. 13, pp. 487–500, June 1997.
[18] D. Zmood and D. G. Holmes, "Stationary frame current regulation of PWM inverterswith zero steady-state error," *IEEE Trans. Power Electron.*, vol. 18, no. 3, pp. 814–822, May 2003.